Molecular modeling of novel 1H-pyrazolo[3,4-b]pyridine derivatives designed as isosters of the antimalarial mefloquine

ARTICLE *in* JOURNAL OF MOLECULAR STRUCTURE THEOCHEM · MARCH 2002

Impact Factor: 1.37 · DOI: 10.1016/S0166-1280(01)00677-7

ELSEVIER

Journal of Molecular Structure (Theochem) 579 (2002) 31–39

THEO CHEM

www.elsevier.com/locate/theochem

Molecular modeling of novel 1*H*-pyrazolo[3,4-*b*]pyridine derivatives designed as isosters of the antimalarial mefloquine

Carla Maria S. Menezes[a,1], Carlos Mauricio R. Sant'Anna[a,b,1], Carlos Rangel Rodrigues[a,1], Eliezer J. Barreiro[a,1,*]

[a]*Laboratório de Avaliação e Síntese de Substâncias Bioativas, Departamento de Fármacos, Faculdade de Farmácia, Universidade Federal do Rio de Janeiro, UFRJ, Cidade Universitária, Ilha do Fundão, CCS, RJ, ZIP-21949-910, BP-68006 Rio de Janeiro, Brazil*

[b]*Departamento de Química, Instituto de Ciências Exatas, Universidade Federal Rural do Rio de Janeiro, UFRRJ, Seropédica, Brazil*

Received 1 May 2001; revised 31 July 2001; accepted 3 August 2001

Abstract

The increasing resistance of *Plasmodium* sp. parasites to the current drugs is the principal reason for the reemergence of malaria. As a consequence, the interest for new and effective drugs against resistant or multidrug-resistant *Plasmodium* strains has increased. This paper describes a molecular modeling study of the new 1*H*-pyrazolo[3,4-*b*]pyridine derivatives (**4** [(3,6-dimethyl-1-phenyl-1*H*-pyrazolo[3,4-*b*]pyridin-4-yl)-(2-piperidinyl)]methanol; **5** [(3-methyl-1-phenyl-6-trifluoromethyl-1*H*-pyrazolo[3,4-*b*]pyridin-4-yl)-(2-piperidinyl)]methanol; **6** [(3,6-dimethyl-1-phenyl-1*H*-pyrazolo[3,4-*b*]pyridin-4-yl)-(2-piridyl)]methanol; **7** 3,6-dimethyl-1-phenyl-4-(2-pyridoyl)-1*H*-pyrazolo[3,4-*b*]pyridine and **8** 3-methyl-1-phenyl-4-(2-pyridoyl)-6-trifluoromethyl-1*H*-pyrazolo[3,4-*b*]pyridine) designed as isosters of the quinoline carbinolamine antimalarial, mefloquine (**2**). The minimal energy conformations of the *erythro* and monoprotonated compounds, obtained by the AM1 semiempirical method, show that the interatomic distances, bond angles and dihedral angles of **4** and **5** are close to those of **2** (AM1 and 3-21G* calculations) and of the X-ray crystal structures of mefloquine salts. The atomic superimposition of **4** and **5** with mefloquine revealed the 1*H*-pyrazolo[3,4-*b*]pyridine system to be coplanar with the mefloquine quinoline ring (RMS = 0.06 Å). Electronic similarities are observed between **4**, **5** and **2** with respect to MEPs, HOMO and LUMO eigenvalues and coefficient distribution, molecular dipole moment and cation–π interaction. Comparable structural and electronic parameters were not observed for **6**–**8**, which can be accounted for by the chemical modifications in the hydroxyl and in the piperidine moieties of the pharmacophore. In a manual docking study performed between **4**–**8** and heme, a probable molecular target of quinoline antimalarial drugs, only **4** and **5** showed the geometrical and energy requirements to effect the biological interaction. The stereoelectronic properties presented here correlate to previous qualitative structure–activity relationships on carbinolamine antimalarials and are in accordance to the recently identified isosteric relationship between the 1*H*-pyrazolo[3,4-*b*]pyridine system and the quinoline nucleus of mefloquine.

Keywords: Mefloquine; Isosterism; 1*H*-Pyrazolo[3,4-*b*]pyridine system; Semiempirical method; Cation–π interaction

1. Introduction

Malaria is considered one of the most important infectious diseases. Millions of people are infected in tropical and sub-tropical areas and the disease causes over one million deaths each year [1,2]. This

* Corresponding author.
E-mail address: eliezer@pharma.ufrj.br (E.J. Barreiro).
[1] LASSBio, http://www.farmacia.ufrj.br/lassbio.

0166-1280/02/$ - see front matter
PII: S0166-1280(01)00677-7

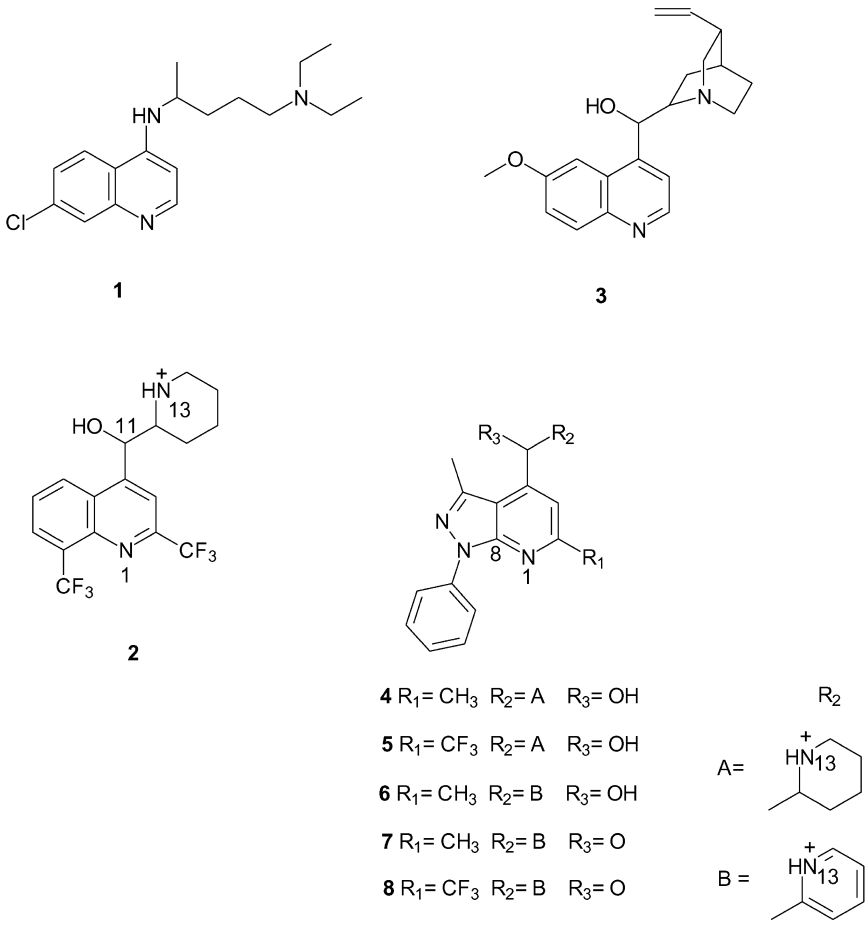

Fig. 1. Chloroquine (**1**), quinine (**3**) and the monoprotonated forms of mefloquine (**2**) and the 1*H*-pyrazolo[3,4-*b*]pyridine compounds (**4**–**8**). Note: Nomenclature of the **4**–**8** 1*H*-pyrazolo[3,4-*b*]pyridine compounds are according to that of mefloquine.

high incidence is primarily due to resistant or multidrug-resistant *Plasmodium* strains, in particular, *P. falciparum* resistance to chloroquine (**1**). The first resistant strains were recognized in the 60s, leading to the USA Walter Reed Army Institute of Research to re-establish its Malaria Research Program with the goal of developing a new antimalarial agent. Mefloquine (**2**), a quinoline carbinolamine, like the first antimalarial quinine (**3**), stood out from about 400 compounds and was launched in the 80s [3]. Nevertheless, resistance to mefloquine has been reported, since its initial use in Africa [4] and southeastern Asia [5,6]. Nowadays, the resistance has increased rapidly in Thailand and adjacent areas and is emerging in Vietnam [7]. Mefloquine is employed in multidrug-resistant *falciparum* malaria treatment and in combination with artemisinin and its derivatives in severe infections as well as a prophylactic agent in prevalent multidrug-resistant *P. falciparum* strains areas [8]. The structures of chloroquine (**1**), mefloquine (**2**) and quinine (**3**) are shown in Fig. 1.

The mechanism of action of quinoline antimalarials, such as mefloquine, is related to the heme metabolism in the protozoa. The heme, or ferriprotoporphyrin IX, is the toxic product from hemoglobin degradation, the process used by the parasite to obtain free essential amino acids. According to the most prevalent theory, quinoline derivatives bind to the heme, interfering on the latter's with its polymerization process [9,10].

The design of new heterocyclic systems such as 1*H*-pyrazolo[3,4-*b*]pyridine can be useful in discovering new lead-compounds in the survey of future antimalarial drugs, especially to treat multidrug-resistant malaria. The 1*H*-pyrazolo[3,4-*b*]pyridine system has been shown to be a bioisoster of heterocyclic systems with distinct biological profiles as anxiolytic [11], antithrombotic [12] and analgesic [13,14].

In this paper, we present a molecular modeling study for mefloquine isosters **4**–**8** (Fig. 1). In vitro biological data revealed **4** and **5** to be active against *P. falciparum* strains whereas **6**–**8**, possessing a ketone and/or a pyridine ring instead of the respective hydroxyl group and piperidine ring observed in **2**, **4** and **5**, were shown to be inactive [15]. These structural differences are in accordance to previous qualitative structure–activity studies [16,17] and suggest that stereoelectronic effects may play a major role in determining biological activity in carbinolamine antimalarial compounds. The structural and electronic features of the monoprotonated forms of the 1*H*-pyrazolo[3,4-*b*]pyridine compounds were analyzed using quantum mechanical methods and compared to those of **2** and/or to the X-ray crystal structures of its salts. In addition, a study was performed in order to compare the **4** and **5** 1*H*-pyrazolo[3,4-*b*]pyridine systems and the quinoline nucleus of **2** as members of cation–π complexes. Finally, a manual docking calculation was performed to predict the putative binding of the 1*H*-pyrazolo[3,4-*b*]pyridine derivatives to the heme at a molecular level.

2. Computational details

The monoprotonated form of the compounds was used in this study due to the acidic internal pH of the food vacuole of the parasite (5.2), the organelle attributed to be the antimalarial locus of action [18]. The structures were built according to the crystalline structure of the hydrochloride and methylsulfonate monohydrate salts of mefloquine [19,20]. The 11*R*,12*S*-*erythro* configuration was attributed to **2**, **4** and **5**, and the *R*-configuration was assigned to C_{11} atom of **6**.[2] The geometry optimization of **2** and of **4**–**8** was performed using the AM1 Hamiltonian within the MOPAC version 7.0 package [21] on an IBM RISC system/6000 workstation with an IBM AIX 3.0 operational system. The structure of **2** was also optimized at the 3-21G* level with the SPARTAN 1.0.5 program (Wavefunction, Irvine, CA, 2000) and compared to the corresponding structure calculated by AM1 as a test for the quality of the semiempirical results. Moreover, previously reported results demonstrated that AM1 is able to generate conformations to mefloquine and its analogues in good agreement with crystalline geometries [22,23]. The dihedral angles $O–C_{11}–C_{12}–N_{13}$ and $O–C_{11}–C_4–C_3$ were independently searched between 0 and 360° in 30° steps. After a reoptimization of the minimal energy conformations with the keywords GNORM = 0.2 and PRECISE, Hessian matrix analysis were employed to unequivocally characterize them as true minima of the potential energy surface. The optimized structures were compared to the mefloquine parameters extracted from the crystal structure of the corresponding methylsulfonate monohydrate salt [20], taking as reference the atoms N_1, C_4, O, C_{11}, C_{12}, N_{13}, C_{14}.

In order to better evaluate the electronic properties of the AM1 minimal energy conformations, they were submitted to a single-point ab initio calculation with a 3-21G* basis set with the SPARTAN 1.0.5 program (Wavefunction Inc. Irvine, CA, 2000). Molecular electrostatic potential maps (MEPs), HOMO and LUMO eigenvalues and orbital coefficients, and the molecular dipole moments were calculated. In this work, the MEPs isoenergy contours were generated in the range from −0.30 to +180.00 kcal/mol and superimposed onto a surface of constant electron density of 0.002 e/au^3. HOMO and LUMO isosurfaces were calculated at 0.0032 a.u. The constants employed in these isosurfaces calculations are default parameters in SPARTAN.

A cation–π interaction study was performed involving 2,8-bis(trifluoromethyl)quinoline (**9**), the quinoline nucleus of **2**, 3,6-dimethyl-1-phenyl-1*H*-pyrazolo[3,4-*b*]pyridine (**10**) and 3-methyl-1-phenyl-6-trifluoromethyl-1*H*-pyrazolo[3,4-*b*]pyridine (**11**), the corresponding 1*H*-pyrazolo[3,4-*b*]pyridine nuclei of active compounds **4** and **5**. The geometry optimizations were carried out using the PM3 method in the SPARTAN 1.0.5 program (Wavefunction, Irvine, CA,

[2] In order to facilitate comparisons, nomenclatures of the **4**–**8** 1*H*-pyrazolo[3,4-*b*]pyridine compounds will be written according to that of mefloquine (see Fig. 1).

Table 1
AM1 calculated structural parameters for the minimal energy conformations of the monoprotonated forms of the **2** and the **4**–**8** 1*H*-pyrazolo[3,4-*b*]pyridine compounds compared to the 3-21G* optimized geometry form and crystal X-ray data of the hydrochloride and methylsulfonate monohydrate of mefloquine

Structural parameters	AM1						3-21G*	Crystal structure	
	2[a]	4[a]	5[a]	6[b]	7	8	2[c]	2[d]	2[e]
Interatomic distances (Å)									
C_{11}–O	1.420	1.421	1.419	1.421	1.223	1.224	1.441	1.414	1.423
O···N_{13}	2.784	2.744	2.786	2.687	3.453	3.551	2.576	2.791	2.730
Bond angles (°)									
C_4–C_{11}–C_{12}	110.7	111.0	110.9	110.5	113.3	114.9	112.06	111.4	110.8
C_4–C_{11}–O	113.9	113.7	114.3	113.4	127.2	126.1	112.73	111.9	111.6
Dihedral angles (°)									
C_4–C_{11}–C_{12}–N_{13}	179.5	− 175.4	178.7	− 133.7	− 57.6	32.2	− 172.46	174.7	− 176.2
O–C_{11}–C_{12}–N_{13}	− 56.6	− 51.4	− 56.7	− 9.1	127.7	− 151.0	− 51.33	− 62.8	− 54.5

[a] *Erythro* form.
[b] 11*R* configuration.
[c] Optmized geometry from 3-21G*.
[d] X-ray diffraction data of the mefloquine methylsulfonate monohydrate.
[e] X-ray diffraction data of the mefloquine hydrochloride.

2000). A twist in the single bond between the phenyl and pyrazole rings was observed in the calculated structures for **10** and **11**, with dihedral angles equal to 28 and 30°, respectively. These results are similar to the dihedral angles determined by crystallographic data for 5-chloro-3-methyl-1-phenyl-4-pyrazolesulphonamide [24] and AM1 calculations of 4-phenyl-3,5-dimethyl-1,7-diphenyl-bis-pyrazolopyridine [25]. The PM3 results are also in agreement with data calculated for a series of 1-phenyl-5-substituted pyrazole derivatives from UV determinations in MeOH solutions [26]. As in the biological environment the 1*H*-pyrazolo[3,4-*b*]pyridine derivatives would be solubilized in water, we feel that the PM3 results are adequate for the kind of problem under consideration in this study, because they reproduce data obtained in a highly polar solvent, which is also able to form strong hydrogen bonds. Moreover, PM3 method has provided binding enthalpies for cation–π interactions in good correlation with experimental values [27]. Calcium ion (Ca^{2+}) was used as a dipositive probe ion because acceptable geometries were obtained with the semiempirical method for the complexes between this ion and the different nuclei analyzed. The initial structures of the complexes were built placing the ion above the centroid of each individual ring of the aromatic moiety. Similar binding enthalpies and geometries were observed for both rings. The binding enthalpies of the complexes were calculated by subtracting the sum of heats of formation of the separated components from the heat of formation of the optimized complexes. The reported data are a result of the interaction of the ion with the benzene ring of 2,8-bis(trifluoromethyl)quinoline (**9**) and with the pyrazole ring of 1*H*-pyrazolo[3,4-*b*]pyridine nucleus of **10** and **11**.

A model of heme was built and the minimal energy conformation superimposed to the heme group from hemoglobin obtained by X-ray crystallography (PDB code 1HAC). The root mean squares (RMS) value between the structures is 0.170 Å. It was also observed that the iron atom is on the same plane of the nitrogen atoms of the porphyrin nucleus, as described in the literature [28]. This model was used on a manual docking study with minimal energy conformations of **4**–**8** using the ESFF force field that is parameterized to iron [29]. The ESFF minimal energy conformations of **4**–**8** are similar to those obtained by AM1. They are positioned above the π-system of the porphyrin nucleus with a distance constraint of 3.5 Å between the quaternary nitrogen atom (N_{13}) and an oxygen atom of the carboxylate group on heme. The interaction enthalpies (IE) were computed by subtracting the sum of heats of formation

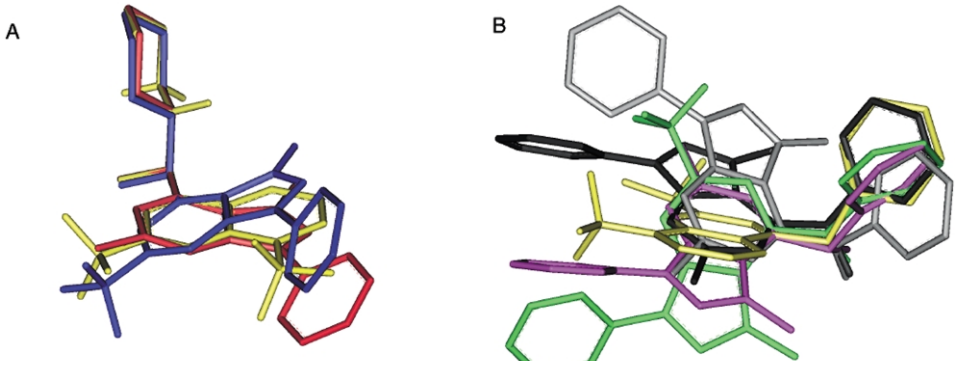

Fig. 2. (A) Stereodiagram of the superimposition of the active compounds **4** (red) and **5** (blue) with mefloquine crystal structure (yellow). (B) Stereodiagram of the superimposition of the inactive compounds **6** (pink), **7** (black) and **8** (gray) with mefloquine crystal structure (yellow). Atoms taken as reference are N_1, C_4, O, C_{11}, C_{12}, N_{13}, C_{14} (see atoms in Fig. 1).

of the separated optimized components from the heat of formation of the optimized complexes [30]. The calculations were performed with the Discover program (Biosym Technologies, San Diego, CA, 1993) on a Silicon Graphics Risk 5000 workstation using the Irix 6.4 operational system.

3. Results and discussion

Interatomic distances, bond angles and dihedral angles of the minimal energy conformers obtained using the AM1 are shown in Table 1. The corresponding 3-21G* optmized geometry for **2** and the X-ray data of the *erythro* racemate forms of the hydrochloride and methylsulfonate monohydrate of mefloquine [19,20] are also presented. The conformation for **2** obtained with AM1 was similar to those obtained with 3-21G* method and to X-ray crystallographic data. This result and previously reported ones [22,23] corroborate the employment of AM1 method in this study.

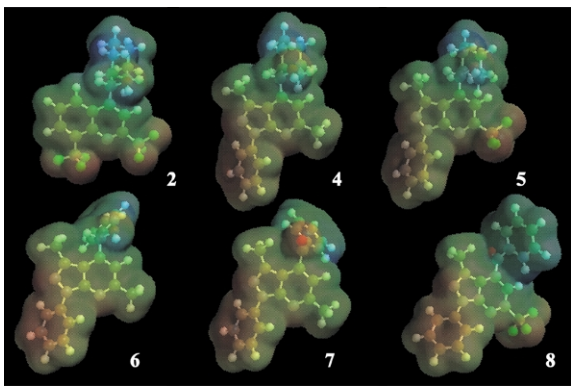

Fig. 3. Molecular electrostatic potential energy isosurfaces superimposed onto total electron density of 0.002 e/a.u.^{3} of the monoprotonated forms of mefloquine (**2**) and the 1*H*-pyrazolo[3,4-*b*]pyridine derivatives (**4**–**8**). The color code is in the range of −0.30 (deepest red) to +180.0 (deepest blue) kcal/mol.

A comparison of the minimal energy conformers of **2** and **4**–**8** with the crystalline data of the mefloquine salts show that the inactive compounds **7** and **8** present different values in relation to the interatomic distances for the C_{11}–O bond and the O···N_{13} interaction, and for the C_4–C_{11}–C_{12} and C_4–C_{11}–O bond angles. The inactive compounds (**6**–**8**) also show very distinct C_4–C_{11}–C_{12}–N_{13} and O–C_{11}–C_{12}–N_{13} dihedral angles. These differences imply a close proximity between the quaternary nitrogen atom N_{13} and the 1*H*-pyrazolo[3,4-*b*]pyridine system, and also the loss of the *gauche* conformation for the O–C_{11}–C_{12}–N_{13} dihedral angle. It is important to note that these differences are observed for parameters related to the N_{13} and O atoms and can be attributed to the chemical modifications of these two atoms that are considered as part of the pharmacophore of carbinolamine antimalarial compounds. These structural results are in agreement with previously reported qualitative structure–activity relationships [16,17] and suggest an explanation for the lack of antimalarial activity for compounds **6**–**8**.

The stereodiagram of the atomic superimposition of compounds **4**–**8** with mefloquine (Fig. 2) shows a

Table 2
Binding enthalpies and ring centroid-Ca^{2+} distances for the complexes of 2,8-bis(trifluoromethyl)quinoline (**9**), 2,6-dimethyl-1-phenyl-1*H*-pyrazolo[3,4-*b*]pyridine (**10**) and 2-methyl-1-phenyl-6-trifluoromethyl-1*H*-pyrazolo[3,4-*b*]pyridine (**11**) with Ca^{2+} *

Complex	Binding enthalpy (kcal/mol)	Ring centroid-Ca^{2+} distances (Å)
9*–Ca^{2+}	− 184.4	4.76
10*–Ca^{2+}	− 182.6	4.15
11*–Ca^{2+}	− 197.1	4.33

* Compounds **9**, **10** and **11** are the nucleus of mefloquine (**2**) compounds **4** and **5**, respectively.

high overlap of **4** and **5**. The **4** and **5** 1*H*-pyrazolo[3,4-*b*]pyridine systems are coplanar to the quinoline ring with a RMS value of 0.06 Å. On the other hand, **6**–**8** show a poor overlap with mefloquine, since the corresponding 1*H*-pyrazolo[3,4-*b*]pyridine systems adopt different planes in relation to that of the aromatic nucleus of mefloquine. These distinct overlaps with mefloquine among the active compounds **4** and **5** and the inactive **6**–**8** can be explained in function of the changes in the pharmacophore, with consequent effect in the biological activity.

The MEPs show that compounds **4** and **5** perfectly match the electrostatic properties of **2** (Fig. 3). The most positive potential is observed in the vicinity of the quaternary nitrogen atom N_{13} whereas the N_1 nitrogen atom presents the less positive potential. In addition, another negative potential is observed near the pyrazole nitrogen N_6 and the *N*-phenyl N_7 atoms, leading to a slightly less negative potential in the 1*H*-pyrazolo[3,4-*b*]pyridine nucleus of **4** and **5** compared to the quinoline ring of **2**. **6**–**8** MEPs also show the vicinity of the quaternary nitrogen atom N_{13} as the most positive potential and the pyridine nitrogen atom N_1 as the region of the less positive potential. An increase in the negative potential on oxygen is also observed for the inactive derivatives. Nevertheless, the MEPS of compounds **6**–**8** do not show a spatial distribution similar to those calculated for **2** and for the active compounds **4** and **5**. Since molecular electrostatic field plays a key role in the recognition process that precedes the formation of the drug-receptor complex, these results may be related to the differences in the biological activity.

The HOMO eigenvalues of compounds **4**–**8** are similar and no relationship could be established with the in vitro activity. The HOMO eigenvalues are calculated in the range of −10.39 to −10.96 eV while that of mefloquine is −12.57 eV. Also, no differences are observed for the HOMO orbitals coefficient distribution. In these compounds, the HOMO orbitals coefficients are strongly localized in the 1*H*-pyrazolo[3,4-*b*]pyridine and the quinoline nucleus, respectively. However, greater differences are observed with respect to their LUMO properties. The active compounds **4** (−0.56 eV) and **5** (−1.44 eV) show higher values than those calculated for the inactive compounds **6** (−2.62 eV), **7** (−3.41 eV) and **8** (−3.80 eV). The mefloquine value is −2.19 eV. Moreover, due to piperidine oxidation, the LUMO coefficients for **6**–**8** are concentrated on the pyridine ring instead of the quinoline and 1*H*-pyrazolo[3,4-*b*]pyridine nucleus as observed for mefloquine and for compounds **4** and **5**, respectively.

The dipole moments of all the compounds studied are smaller (15.41–18.01 D) than that of **2** (19.07 D), suggesting that there should be no relation between this parameter and the observed differences in the antimalarial activity.

In order to better analyze the electronic similarities between the 1*H*-pyrazolo[3,4-*b*]pyridine nucleus of **4** and **5** and the 2,8-bis(trifluoromethyl)quinoline moiety (**9**) of **2**, we evaluated their cation–π complexes with a divalent cation, Ca^{2+}. Cation–π interaction has been recognized as an important non-covalent stabilizing force between cations and aromatic π-electrons systems involved in biological recognition processes such as drug-receptor or enzyme–substrate interactions [31]. The aromatic nucleus was elected for the binding enthalpy calculations of the complexes due to the structural similarity of the compounds analyzed (**2**, **4** and **5**). According to PM3 results, the 1*H*-pyrazolo[3,4-*b*]pyridine nucleus of the active compounds **4** and **5**, 3,6-dimethyl-1-phenyl-1*H*-pyrazolo[3,4-*b*]pyridine (**10**) and 2-methyl-1-phenyl-6-trifluoromethyl-1*H*-pyrazolo[3,4-*b*]pyridine (**11**), respectively, show binding enthalpies (Table 2) and geometric features (Fig. 4) comparable to those of the quinoline nucleus of mefloquine (**9**). In all complexes, the Ca^{2+} is located near the lone pair electrons of the pyridine nitrogen atom (N_1); it also interacts with the phenyl and methyl groups in the complex with **10** or the trifluoromethyl group in the

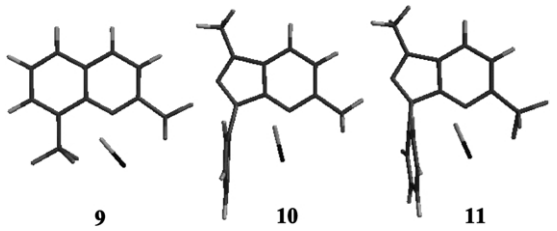

Fig. 4. The optimized geometries for complexes of **9**–**11** with Ca^{2+}.

complex with **11** or the two trifluoromethyl groups in the complex with **9**. A comparable geometry for the Ca^{2+}-2,8-bis(trifluoromethyl)quinoline complex was reported by Bhattacharjee employing the 3-21G* method [32]. In addition, the distances between the ring centroid and the Ca^{2+} ion are very close for the different nuclei (Table 2). These results suggest that the proposed 1*H*-pyrazolo[3,4-*b*]pyridine nucleus is able to achieve cation–π interactions with similar geometric and energetic features of mefloquine nucleus.

Recently, Bachhawat et al. [33] revised the molecular interaction of quinoline antimalarial drugs with the heme. Based on isothermal titration calorimetry, it is suggested that the first interaction involves an electrostatic binding between the quaternary nitrogen atom of antimalarials and an oxygen atom of the carboxylate group on heme. Following that, a typical hydrophobic interaction takes place, considered as the predominant force between the quinoline nucleus and the planar porphyrin system. This experimental model is corroborated by molecular modeling on tebuquine analogues [34] and was adopted in the present study.

A manual docking study was carried out to evaluate the energy and geometry of interaction of the complexes composed by the compounds **4**–**8** and the heme. The calculated IE are shown in Table 3, together with the distances involving the quaternary nitrogen atom N_{13} and an oxygen atom of the carboxylate group on heme, and the quinoline carbon C_8 and the iron atom. The in vitro antimalarial activity data [15] are also presented for a comparison with the modeling results.

Although a direct correlation with the biological activity could not be established, it can be seen that the IE are very different between the active and inactive compounds (Table 3). The IE calculated values show that compounds **4**–**5** have the strongest interactions with heme (−120 to −130 kcal/mol), which suggests a relationship between the force of interaction and the in vitro antimalarial activity. The distances between the quaternary nitrogen atom (N_{13}) and an oxygen atom of the carboxylate group on heme (3.10–3.58 Å) suggest that the interaction is essentially electrostatic (Fig. 5), as previously shown by experimental calorimetric method [33]. Similar results were observed for tebuquine analogues [34]. Nevertheless, the distance from the 1*H*-pyrazolo[3,4-*b*]pyridine nucleus to that of porphyrin (C_8-iron atom) is different for the active and inactive series (Fig. 5). The calculated distances for compounds **4** and **5**, 3.41 and 3.20 Å, respectively, are closer to those for hydrophobic interactions. Higher distances were observed

Table 3
Calculated interaction enthalpies (IE), selected structural parameters and in vitro biological activity for the 1*H*-pyrazolo[3,4-*b*]pyridine compounds–heme complexes

Compound	IC_{50}[a] (μg/l)		IE (kcal/mol)	Distance (Å)	
	D-6 clone[b]	W-2 clone[c]		$^{+}N_{13}H–COO^{-}$	C_8-iron atom
4	10.2	13.6	− 120.20	3.41	3.12
5	15.6	32.0	− 127.72	3.20	3.04
6	ND[d]	ND[d]	− 89.72	3.54	5.42
7	1700	5600	− 74.68	3.48	5.11
8	ND[d]	1350	− 64.41	3.58	4.85

[a] Fifty percent inhibitory concentration.
[b] Chloroquine-sensitive and mefloquine-resistant *P. falciparum* clone.
[c] Chloroquine-resistant and mefloquine-sensitive *P. falciparum* clone.
[d] Not detected.

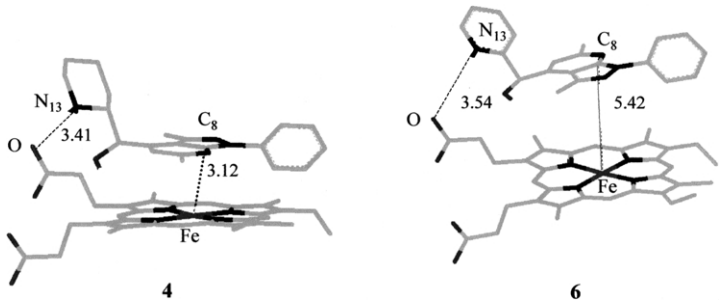

Fig. 5. Lowest energy complexes with heme for compounds **4** (active) and **6** (inactive). The distances (Å) $^{+}N_{13}H–COO^{-}$ and C_8–Fe are also showed. Hydrogen atoms were removed to improve visualization.

for the inactive compounds **6**–**8** (4.85–5.42 Å). This could prevent the occurrence of the π–π stacking between the compounds and the subsequent biological effect. These results are a consequence of geometric differences of compounds **6**–**8** in relation to mefloquine, which could result in modifications in the pharmacophore.

4. Conclusions

The interatomic distances, bond angles and dihedral angles of the active compounds **4** and **5** were shown to be closer to those from mefloquine by means of the AM1 method. Superimposition of models to mefloquine shows that the 1*H*-pyrazolo[3,4-*b*]pyridine systems of compounds **4** and **5** are coplanar to the quinoline nucleus of mefloquine. According to 3-21G* single point calculations, electronic features such as MEPs, HOMO and LUMO eigenvalues and orbital coefficients, and molecular dipole moments were also comparable to those from mefloquine. Similar binding enthalpies and geometries are observed for the aromatic nucleus of mefloquine (**9**) and for the 1*H*-pyrazolo[3,4-*b*]pyridine systems of **10** and **11** with respect to the cation–π interaction with Ca^{2+}. Different mefloquine structural and electronic properties are observed for the inactive compounds **6**–**8**. Likewise, geometric and electronic features allow **4** and **5** to establish similar binding to heme as reported for antimalarial drugs. These calculated differences between the active and inactive compounds can be attributed to stereoelectronic changes in the pharmacophore brought about the oxidation of the hydroxyl group to a ketone function (**7** and **8**) and/or the oxidation of the piperidine ring to pyridine (**6**–**8**). In short, the molecular modeling study suggests a stereoelectronic interpretation for previous qualitative structure–activity relationships on carbinolamine antimalarial compounds and corroborate the in vitro biological assay that indicated the 1*H*-pyrazolo[3,4-*b*]pyridine nucleus as an isoster system of the quinoline nucleus of mefloquine.

Acknowledgements

This research has received financial support from Brazilian agencies CNPq, CAPES, FAPERJ, FUJB and PRONEX.

References

[1] HIV, TB and malaria — three major infectious diseases threats, WHO Information, Fact Sheets Backgrounder No. 1, July 2000, http://www.who.int/ in 2000-03-21.
[2] Malaria, WHO Information, Fact Sheets No. 94, revised in October 1998, http://www.who.int/ in 2000-03-21.
[3] D.A. Casteel, Antimalarial agents, in: M.E. Wolff (Ed.), 5th ed, Burger's Medicinal Chemistry and Drug Discovery, vol. 5, Wiley, New York, 1997, pp. 5–91.
[4] R. Félix, F. Gay, A. Lyocoubi, M.D.G. Bustos, B. Diquet, M. Danis, M. Gentilini, Bull. Soc. Pathol. Exot. 83 (1990) 43.
[5] E.L. Boudreau, H.K. Webster, K. Pavanand, L. Thoshinga, Lancet ii (1982) 1335.
[6] J.J. Karwacki, H.K. Webster, N. Limsomwong, G.D. Shanks, Trans. R. Soc. Trop. Med. 83 (1989) 152.
[7] J.A. Simpson, E.R. Watkins, R.N. Price, L. Aarons, D.E. Kyle, N.J. White, Antimicrob. Agents Chemother. 44 (2000) 3414.
[8] World Health Organization, WHO model prescribing information: drugs used in parasitic diseases, 2nd ed, WHO, Geneva, 1995 pp. 24–45.

[9] G. Padmanaban, P.N. Rangarajan, Biochem. Biophys. Res. Commun. 268 (2000) 665.
[10] D.J. Sullivan, H. Matile, R.G. Ridley, D.E. Goldberg, J. Biol. Chem. 273 (1998) 31,103.
[11] T.M. Bare, C.D. McLaren, J.B. Campbell, J.W. Firor, J.F. Resch, C.P. Walters, A.I. Salama, B.A. Meiners, J.B. Patel, J. Med. Chem. 32 (1989) 31103.
[12] A.S. Carvalho, C.A.M. Fraga, K.C.M. Silva, A.L.P. Miranda, E.J. Barreiro, J. Braz. Chem. Soc. 7 (1996) 247.
[13] L.R.S. Dias, M.J.F. Alvim, A.C.C. Freitas, E.J. Barreiro, A.L.P. Miranda, Pharm. Acta Helv. 69 (1994) 163.
[14] M.A. Gaston, L.R.S. Dias, A.C.C. Freitas, A.L.P. Miranda, E.J. Barreiro, Pharm. Acta Helv. 71 (1996) 213.
[15] R.S. Dias, A.C.C. Freitas, E.J. Barreiro, D.K. Goins, D. Nanayakkara, J.D. Mc-Chesney, Boll. Chim. Farmac. 130 (2000) 14.
[16] C.J. Ohnmacht, A.R. Patel, R.E. Lutz, J. Med. Chem. 14 (1971) 926.
[17] D.W. Boykin Jr., A.R. Patel, R.E. Lutz, J. Med. Chem. 11 (1968) 273.
[18] A. Yayon, K.I. Cavantchick, H. Ginsburg, EMBO J. 30 (1984) 2695.
[19] J.M. Karle, I.L. Karle, Acta Crystallogr. C47 (1991) 2391.
[20] J.M. Karle, I.L. Karle, Antimicrob. Agents Chemother. 35 (1991) 2238.
[21] J.J.P. Stewart, MOPAC 7.0, Frank J. Seiler Research Laboratory, US Air Force Academy, Colorado Springs, 1993.
[22] A.K. Bhattacharjee, J.M. Karle, J. Med. Chem. 39 (1996) 4622.
[23] A.K. Bhattacharjee, J.M. Karle, Bioorg. Med. Chem. 6 (1998) 1927.
[24] J. Iulek, J. Zukerman-Schpector, E.J. Barreiro, A.C.C. Freitas, Acta Crystallogr. C49 (1993) 1015.
[25] A.B.J. Parusel, R. Schamschule, D. Piorun, K. Rechthaler, A. Puchala, D. Rasala, K. Rotkiewicz, G. Köhler, J. Mol. Struct. (Theochem) 419 (1997) 63.
[26] S. Tabak, I.I. Grandberg, A.N. Kost, Tetrahedron 22 (1965) 2703.
[27] C.M.R. Sant'Anna, R.B. Alencastro, E.J. Barreiro, J. Mol. Struct. (Theochem) 429 (1998) 217.
[28] M.F. Perutz, G. Fermi, B. Luisi, Acc. Chem. Res. 20 (1987) 309.
[29] S. Barlow, A.L. Rohl, D. O'Hare, Chem. Commun. 2 (1996) 257.
[30] Ajay, M.A. Murcko, J. Med. Chem. 38 (1995) 4953.
[31] J.C. Ma, D.A. Dougherty, Chem. Rev. 97 (1997) 1303.
[32] A.K. Battacharjee, J. Mol. Struct. (Theochem) 529 (2000) 193.
[33] K. Bachhawat, C.J. Thomas, N. Surolia, A. Surolia, Biochem. Biophys. Res. Commun. 276 (2000) 1075.
[34] P.M. O'Neill, D.J. Willock, S.R. Hawley, P.G. Bray, R.C. Storr, S.A. Ward, B.K. Park, J. Med. Chem. 40 (1997) 437.